Immunity
Article

Antigen Ligation Triggers a Conformational Change within the Constant Domain of the αβ T Cell Receptor

Travis Beddoe,[1] Zhenjun Chen,[2] Craig S. Clements,[1] Lauren K. Ely,[1] Simon R. Bushell,[1] Julian P. Vivian,[1] Lars Kjer-Nielsen,[2] Siew Siew Pang,[1] Michelle A. Dunstone,[1] Yu Chih Liu,[1] Whitney A. Macdonald,[1] Matthew A. Perugini,[3] Matthew C.J. Wilce,[1] Scott R. Burrows,[4] Anthony W. Purcell,[3] Tony Tiganis,[1] Stephen P. Bottomley,[1] James McCluskey,[2,5,*] and Jamie Rossjohn[1,5,*]

[1]Protein Crystallography Unit, Department of Biochemistry and Molecular Biology, School of Biomedical Sciences, Monash University, Clayton, Victoria 3800, Australia
[2]Department of Microbiology and Immunology
[3]Department of Biochemistry and Molecular Biology, The Bio21 Molecular Science and Biotechnology Institute University of Melbourne, Parkville, Victoria 3010, Australia
[4]Division of Infectious Diseases and Immunology, Queensland Institute of Medical Research, Brisbane 4029, Australia
[5]These authors contributed equally to this work
*Correspondence: jamesm1@unimelb.edu.au (J.M.), jamie.rossjohn@med.monash.edu.au (J.R.)
DOI 10.1016/j.immuni.2009.03.018

SUMMARY

Ligation of the αβ T cell receptor (TCR) by a specific peptide-loaded major histocompatibility complex (pMHC) molecule initiates T cell signaling via the CD3 complex. However, the initial events that link antigen recognition to T cell signal transduction remain unclear. Here we show, via fluorescence-based experiments and structural analyses, that MHC-restricted antigen recognition by the αβ TCR results in a specific conformational change confined to the A-B loop within the α chain of the constant domain (Cα). The apparent affinity constant of this A-B loop movement mirrored that of αβ TCR-pMHC ligation and was observed in two αβ TCRs with distinct pMHC specificities. The Ag-induced A-B loop conformational change could be inhibited by fixing the juxtapositioning of the constant domains and was shown to be reversible upon pMHC disassociation. Notably, the loop movement within the Cα domain, although specific for an agonist pMHC ligand, was not observed with a pMHC antagonist. Moreover, mutagenesis of residues within the A-B loop impaired T cell signaling in an in vitro system of antigen-specific TCR stimulation. Collectively, our findings provide a basis for the earliest molecular events that underlie Ag-induced T cell triggering.

INTRODUCTION

T cells orchestrate specific immunity through antigen (Ag) recognition via specific αβ or γδ T cell receptors (TCRs). The majority of T cells express an αβ TCR that recognizes peptide-laden major histocompatibility complex (pMHC) class I and class II molecules (Rudolph et al., 2006), whereas natural killer T cells (NKT cells) express a semi-invariant αβ TCR that interacts with lipid-laden CD1d molecules (Borg et al., 2007). MHC-restricted TCR ligation is central to the adaptive immune response and results in a signal being transmitted to the T cell that activates a program of effector function and proliferative expansion of Ag-specific, naive T cells. Each chain of the αβ TCR heterodimer is composed of a variable (V) and a constant (C) ectodomain. The V domains, which interact with Ag via the complementarity determining regions (CDRs), show considerable diversity (Turner et al., 2006), and this is manifested in the different modes of interaction between TCRs and pMHC ligands, notwithstanding some generalities in TCR-pMHC docking (Clements et al., 2006; Feng et al., 2007; Rudolph et al., 2006; Tynan et al., 2005).

Despite these diverse TCR-pMHC structural landscapes, Ag ligation leads to T cell signaling, yet the TCR does not possess intracellular signaling domains, and as such antigen recognition is disassociated from T cell signaling. Instead, the αβ and γδ TCRs are noncovalently coupled to the conserved multisubunit signaling apparatus, comprising the CD3εγ and CD3εδ heterodimers and the ζζ homodimer (Kane et al., 2000). Although the TCR-CD3 interactions are mediated via their respective transmembrane regions, the interactions between their ectodomains are considered to contribute to TCR-CD3 specificity (Call and Wucherpfennig, 2004, 2005; Call et al., 2004). In mice and humans, it appears that the dominant stoichiometry of the complex comprises one αβ TCR, one CD3εγ heterodimer, one CD3εδ heterodimer, and one ζζ homodimer although higher-order stoichiometries are also reported in T cells (Schamel et al., 2005), and moreover the stoichiometry differs in γδ TCR-CD3 complexes (Hayes and Love, 2006). Although structures of isolated CD3 components have been determined (Arnett et al., 2004; Kjer-Nielsen et al., 2004; Sun et al., 2001, 2004), the precise nature of the interaction between the TCR and the CD3 complex is unknown, although it is clear that the monomorphic CD3 subunits interact with the constant and transmembrane domains of the TCR (Call et al., 2004; Kuhns and Davis, 2007). Moreover, different schemes have been proposed to explain the mechanism by which TCR ligation is directly communicated to the signaling apparatus. The current dogma favors a model whereby clustering of TCRs concentrates the signaling units and associated kinases to achieve a threshold of signaling via receptor

phosphorylation (Alarcon et al., 2006; Choudhuri et al., 2005). Nonetheless, there is also tantalizing evidence that the earliest TCR signaling event involves binding of the adaptor protein Nck to a proline-rich region in the cytoplasmic tail of CD3ε that is exposed by a change in the TCR-CD3 conformation (Alarcon et al., 2006; Choudhuri et al., 2005). Moreover, a role for the proline-rich region in the $CD4^+CD8^+$ developmental stage has recently been reported (Mingueneau et al., 2008). However, evidence for a conformationally transmitted signal through the TCR ectodomains remains elusive, not the least because of the inherent challenge of unambiguously demonstrating a link between any conformational change in the TCR and subsequent signaling. This is especially difficult given the likely role of TCR aggregation regardless of the earliest signaling event. Accordingly, a key step in making a connection between any conformational change and signaling is the demonstration of a dynamic, ligand-induced conformational change in a region of the TCR likely to impact on CD3 structure in the manner described by Alarcon and colleagues (Gil et al., 2002, 2005; Minguet et al., 2007; Risueno et al., 2005).

Fluorescence-based approaches for detecting real-time conformational change in proteins are a well-established technique (Cohen et al., 2005; Johnson, 2005; Kobilka and Gether, 2002) and moreover represent the most sensitive spectroscopic technique available because it requires small amounts of sample yet produces a high signal to noise ratio even in complex mixtures. In addition there are many commercial fluorophores available that have unique chemical properties, which can be used to measure conformational change. To address the central question of whether Ag-induced conformational change within the ectodomain of a TCR underscores the basis of T cell triggering, we adopted a site-directed fluorescence labeling (SDFL) approach, whereby we engineered unique cysteine residues into the TCR and specifically labeled the TCR with a thiol-reactive fluorescent dye. Collectively, our studies demonstrate that pMHC ligation leads to a specific conformational change within the constant domain of the TCR, suggesting a basis for the earliest molecular events that underlie T cell triggering.

RESULTS

Structural Data

Intracellular signaling via cell surface receptors can proceed by a number of distinct mechanisms, which include ligand-induced oligomerization, higher-order aggregation, and induced conformational changes. Much like immunoglobulin ligation on B cells, the initial structural data on TCR-pMHC complexes suggested no conformational change within the TCR C domain upon Ag ligation, and as such T cell-triggering models that invoked a conformational change in the TCR upon Ag ligation were discounted; however, this initial evidence relied on very few TCRs for which unliganded and ligated structures could be directly compared. Moreover, the relatively low resolution of TCR-pMHC complexes, crystal-packing effects, the poorly resolved electron density of the C domains in some TCR-pMHC complexes, and the large number of TCR-pMHC complexes determined in which the C domains were absent (Rudolph et al., 2006) could have masked any conformational changes within the constant domain. Given that the TCR structural database is now more extensive (Table S1 available online; Clements et al., 2006; Godfrey et al., 2008; Gras et al., 2008), we re-evaluated this initial contention. Analysis of the structural data of unliganded and ligated αβ TCRs suggests the propensity for the A-B loop (residues 129 to 136) of the Cα domain to exist in two conformational states that are correlated with the ligation state of the TCR. Moreover, these differing conformational states of the A-B loop have been observed in αβ TCRs interacting with pMHC-I, pMHC-II, and CD1d-lipid complexes (Supplemental Data). This conformational change was observed in the well-described LC13 TCR system where the A-B loop points toward the Cβ β sheet in the unliganded state and appears to represent a "closed" conformation whereas upon ligation with HLA-B8-FLRGRAYGL ($HLA\text{-}B8^{FLR}$), the A-B loop adopts an "open" conformation in that it moves away from the Cβ domain (Figures 1A–1D; Kjer-Nielsen et al., 2002a). The A-B loop, which is rich in positively charged residues, projects into a cavity of the Cβ domain and was initially proposed as a binding site for the negatively charged CD3εγ (Ghendler et al., 1998; Wang et al., 1998). However, recent mutagenesis studies support an alternate model in which Cα D-E and Cβ C-C' loops of αβ TCR interact with CD3εδ and CD3γε, respectively, allowing TCR-CD3εδ interactions to stabilize CD3γε within the complex (Kuhns and Davis, 2007). In both models, the interaction of TCR-CD3 is suggested to engender a rotational or piston-like displacement of the CD3 components upon Ag ligation that is transmitted through the TCR to initiate signaling. Hence, a ligation-induced movement in the A-B loop of Cα could potentially facilitate or guide this rearrangement or promote TCR dimerization, and is consistent with a conformation-dependent model of T cell triggering. Such a model would also be consistent with the ligand-induced binding of Nck to the cytoplasmic tail of CD3ε reflecting a change in the TCR-CD3 conformation. Moreover, the role of this conformational change does not preclude the importance of TCR-CD3 clustering and rearrangement of components within this complex. Thus, the structural changes in the Cα domains of liganded versus unliganded TCRs suggested to us that this Ag-induced conformational change was a potential first step in initiating T cell triggering through such a mechanism.

Molecularly Tagging the Cα A-B Loop with Fluorochromes

Given that a mutagenesis approach is limited in its ability to discriminate the role of CD3 components in TCR assembly and transport versus their role in Ag-mediated signaling, we adopted a more direct biochemical approach to address the central question of whether Ag ligation of the TCR led to a dynamic and discrete change in the conformation of the A-B loop in a biochemical system. Site-directed fluorescence labeling (SDFL) permitted examination of the conformational change within the TCR Cα A-B loop upon ligation with specific antigen, $HLA\text{-}B8^{FLR}$. Many fluorescent dyes are sensitive to water and their emission properties change dramatically upon moving from an aqueous to a nonaqueous environment, and such approaches have been used previously in other biological systems to reveal conformational change and change of environment in protein structure (Shatursky et al., 1999; Shepard et al., 1998). The dye we employed, *N,N'*-dimethyl-*N-(iodoacetyl)-N'*-(7-nitrobenz-2-oxa-1,

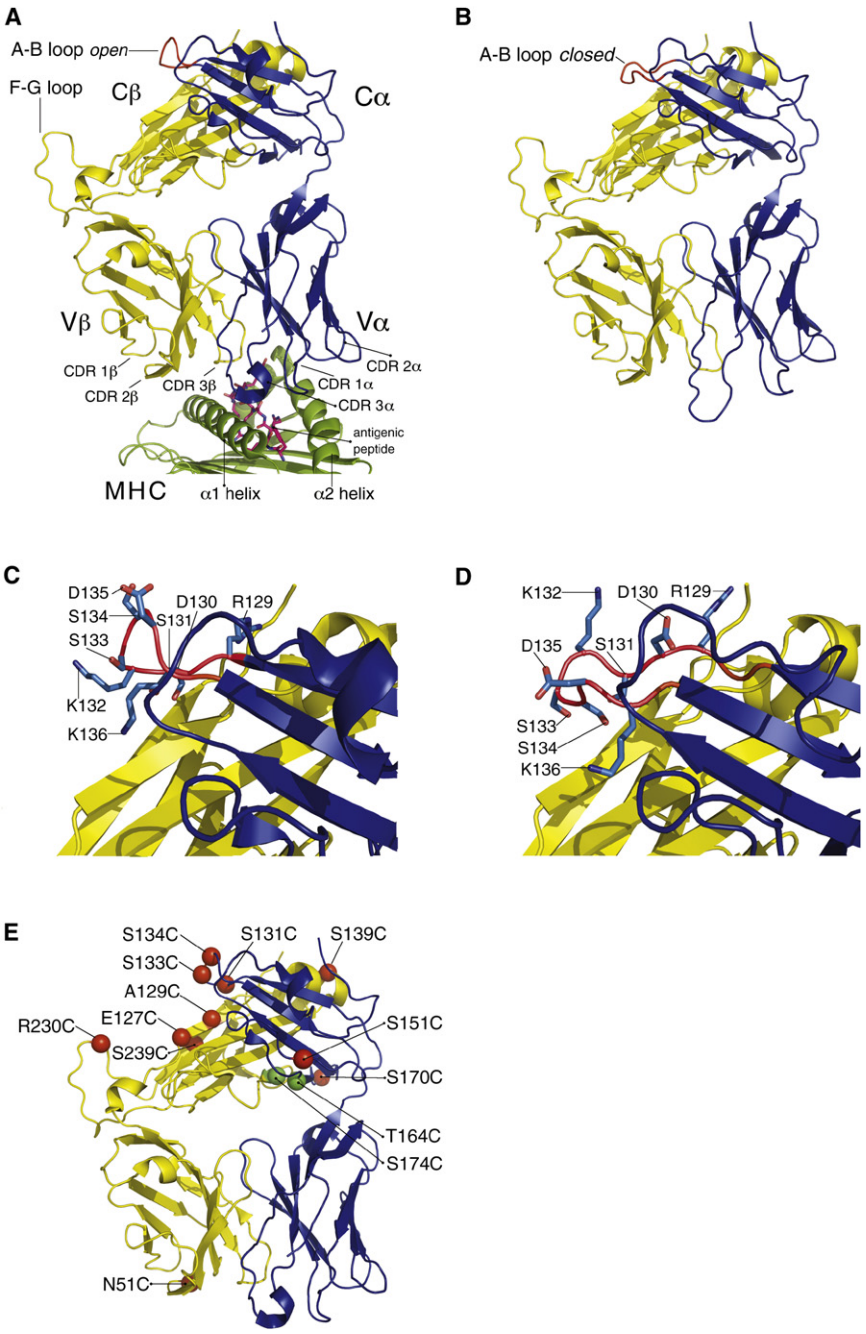

Figure 1. Structures of the Liganded and Unliganded-LC13 TCR

(A) The "open" conformation of LC13 TCR in complex with HLA-B8 (PDB accession code 1MI5) (Kjer-Nielsen et al., 2002b). The MHC molecule is represented as a cartoon and colored green. The antigenic peptide is shown in stick format with the carbon atoms colored magenta. The heterodimeric TCR is colored by chain with the α chain represented in blue and the β chain in yellow. The variable and constant domains within each chain are labeled Vα,Vβ and Cα,Cβ, respectively. The positions of the CDR loops and the F-G loop are indicated. The position of the A-B loop is indicated and highlighted in red. In this "open" conformation, the A-B loop projects away from the Cβ domain.

(B) The "closed" conformation of LC13 TCR as observed in the crystal structure of the unliganded-TCR (PDB accession code 1KGC) (Kjer-Nielsen et al., 2003). The figure is colored similarly as in (A). The "closed" conformation of the A-B loop is distinct from the "open" conformation in that the A-B loop projects toward the Cβ domain.

(C and D) Close-up view of the A-B loop, colored red, in the open (C) and closed (D) conformations. The side chains of the residues in the A-B loop are displayed in stick format.

(E) Cartoon representation of the LC13 TCR structure colored by chain as detailed in (A). The positions of the residues mutated to cysteines to enable the connection of the fluorescent probes are indicated and depicted as red spheres. The position of the cysteine mutations that introduce a disulfide bond between the Cα and Cβ domains of the TCR, to produce the dsTCR, are labeled and shown as green spheres.

3-diazol-4yl)ethylenediamine (IANBD), has a relatively small size and is uncharged, but possesses a polar characteristic that enables it to be soluble in aqueous environment (Haugland, 1996). The emission of NBD is strongly quenched by water and thus NBD fluorescence intensity increases when the dye moves from aqueous to nonaqueous environment (Crowley et al., 1994). To validate the suitability of this targeted NBD fluorescence-based approach in a TCR-pMHC system, we first introduced a cysteine mutation in the CDR2β loop of the LC13 TCR (Asn51β Cys) and labeled it with NBD (see Experimental Procedures) (Figure 1E). We have previously shown that the LC13^{N51C} substitution does not affect the binding to HLA-B8^{FLR} despite the role of this region at the Ag interface (Borg et al., 2005). The typical fluorescence emission spectrum of LC13$^{N51C\text{-}NBD}$ is shown (Figure 2A). Upon addition of increasing amounts of the HLA-B8^{FLR}, the emission spectra showed a substantial increase of fluorescence intensity at 535 nm (Figure 2A), suggesting a release of water from the binding interface upon ligation, which is consistent with the biophysical analysis of the LC13-HLA-B8^{FLR} interaction (Ely et al., 2006). However, there was no change in fluorescence intensity when an irrelevant HLA-B8-restricted epitope, RAKFKQLL (HLA-B8^{RAK}), was used (Figure 2B), indicating that the change in fluorescence intensity is attributable to specific binding to HLA-B8^{FLR}. Binding of HLA-B8^{FLR} to LC13$^{N51C\text{-}NBD}$ showed a clear dose dependence (Figure 2B). By fitting the data points, a single-site hyperbolic function showed that equilibrium affinity of the HLA-B8^{FLR}-LC13$^{N51C\text{-}NBD}$ interaction was 4.16 ± 0.71 μM (Figure 2B; Table 1). The TCR-pMHC affinity measured with the NBD probe is nearly identical to that determined by monitoring tryptophan fluorescence upon LC13-HLA-B8^{FLR} ligation (Ely et al., 2005) and closely matches the binding affinity as judged

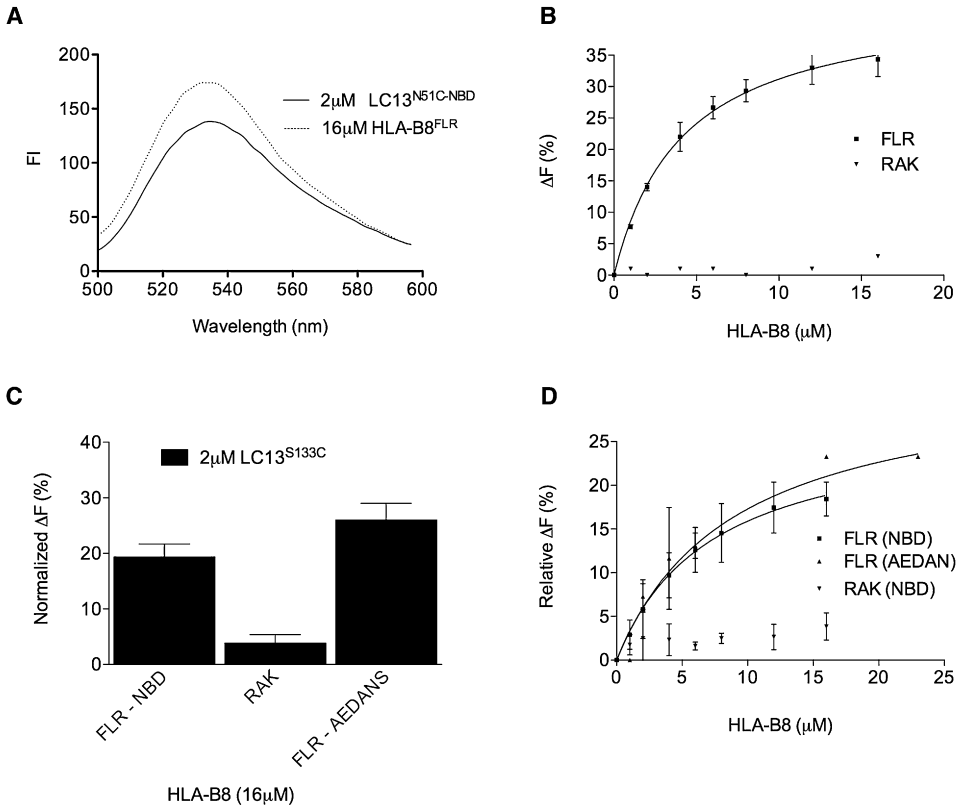

Figure 2. Change in Fluorescence of Intensity of NBD Attached to Cysteine Substituted at Position 51 and S133 of LC13

(A) The fluorescence emission of $LC13^{N51C\text{-}NBD}$ (solid line) when titrated with increasing concentration of $HLA\text{-}B8^{FLR}$ (16 μM) (dotted line).

(B) The change of fluorescence emission of $LC13^{N51C\text{-}NBD}$ at 535 nm at each concentration of HLA-B8-peptide complex was fitted to a single-site binding model (solid line). The percentages of changes are means ± SE (n = 3).

(C) The change in fluorescence emission at 535 nm related as percentage (see Experimental Procedures) of $LC13^{S133C\text{-}NBD}$ is clearly present at 16 μM $HLA\text{-}B8^{FLR}$ where there is little change in fluorescence in the presence of 16 μM $HLA\text{-}B8^{RAK}$.

(D) The percentage change of fluorescence of $LC13^{S133C\text{-}AEDANS}$ and $LC13^{S133C\text{-}NBD}$ was fitted to a single-site binding model.

by surface plasmon resonance (Borg et al., 2005), suggesting that this approach is well suited for probing other conformational changes in the LC13 TCR (Table 1).

Conformational Movement of the A-B Loop

To establish whether $HLA\text{-}B8^{FLR}$ ligation to the LC13 TCR led to a conformational change in the A-B loop, a serine at position 133 was substituted to cysteine ($LC13^{S133C}$) and labeled with NBD ($LC13^{S133C\text{-}NBD}$) (Figure 1C). The fluorescence emission spectrum of $LC13^{S133C\text{-}NBD}$ is similar to that of $LC13^{N51C\text{-}NBD}$, suggesting that the NBD moiety is in an aqueous environment (data not shown), which is consistent with the location of this residue in the crystal structure (Figure 1C). The fluorescence intensity of $LC13^{S133C\text{-}NBD}$ changed approximately 20% upon the addition of increasing amounts of $HLA\text{-}B8^{FLR}$ (Figure 2C), suggesting that the A-B loop changed conformation upon Ag ligation. This change in fluorescence intensity was not observed when similar concentrations of $HLA\text{-}B8^{RAK}$ were added, revealing that the conformational change of the A-B loop occurs only upon MHC-restricted Ag ligation (Figure 2C). In seven independent experiments, there was clearly an Ag-dependent dose change in fluorescence intensity of $LC13^{S133C\text{-}NBD}$ upon $HLA\text{-}B8^{FLR}$ titration, as reported by the proposed conformational change in the A-B loop (Figure 2D). By fitting the data points to a single site, hyperbolic function showed that equilibrium affinity of $LC13^{S133C\text{-}NBD}$ interaction with $HLA\text{-}B8^{FLR}$ is Kd of 7.22 ± 3.54 μM, which is very similar to the affinity reported by $LC13^{N51C\text{-}NBD}$-positioned probe (Table 1), indicating that the conformational change of the A-B loop is the result of Ag ligation.

The physio-chemical properties of some fluorescent probes can occasionally lead to their burial into an environment irrespective of conformation of the native unmodified protein (Valeva et al., 1996). To discount this possibility in monitoring the A-B loop movement, a different fluorescent probe, 5-((((2-iodoacetyl)amino)ethyl)amino)naphthalene-1-sulfonic acid (IAEDANS), was attached to $LC13^{S133C}$. AEDANS is an environmentally sensitive probe, yet it has different physio-chemical properties compared to NBD (Haugland, 1996). The typical emission spectrum of $LC13^{S133C\text{-}AEDANS}$ (data not shown) shows that AEDAN probe has a wavelength maximum at 480 nm. Upon titration of increasing concentration of $HLA\text{-}B8^{FLR}$ against $LC13^{S133C\text{-}AEDANS}$, there was an approximately 25% change in fluorescence intensity of the probe (data not shown). The calculation of the apparent equilibrium affinity constant (Kd) from the change of fluorescence intensity was 8.95 ± 3.73 μM (Figure 2D; Table 1), which matched closely to the Kd that was

Table 1. The Affinity of Interaction between TCR and Its Cognate pMHC Determined by Change of Fluorescence Intensity

TCR Mutant	KD (μM)
LC13 WT	12.5 (Borg et al., 2005)
LC13 WT	5.5 (Ely et al., 2005)
$LC13^{N51C\text{-}NBD}$	4.16 ± 0.71
$LC13^{S133C\text{-}NBD}$	7.22 ± 3.54
$LC13^{S133C\text{-}AEDAN}$	8.95 ± 3.73
$LC13^{S131C\text{-}NBD}$	6.88 ± 1.99
$LC13^{S134C\text{-}NBD}$	1.56 ± 0.40
$LC13^{E127C\text{-}NBD}$	ND
$LC13^{A129C\text{-}NBD}$	ND
$LC13^{R230C\text{-}NBD}$	ND
$LC13^{S239C\text{-}NBD}$	ND
$LC13^{S139C\text{-}NBD}$	ND
$LC13^{S151C\text{-}NBD}$	ND
$LC13^{S170C\text{-}NBD}$	ND
A6 WT	0.82 (Ding et al., 1999)
$A6^{S133C\text{-}NBD}$	0.80 ± 0.22

ND, not determined.

determined with the NBD probe. There have been various conflicting reports describing the propensity of TCRs to dimerize in solution (Baker and Wiley, 2001; Deng et al., 2007), as well as the observation of crystallographic TCR dimers (Tynan et al., 2005), and our fluorescence-based observations may have been attributable to such factors. To evaluate this possibility, analytical ultracentrifugation (AUC) studies were undertaken on the LC13 TCR in the nonligated and ligated state, which revealed that the LC13 TCR and the LC13 TCR-HLA-$B8^{FLR}$ complex remained monomeric in solution, even at very high protein concentrations (data not shown). These studies indicated that the conformational change in A-B loop in the LC13 TCR is probe independent and is exquisitely linked to MHC-restricted Ag ligation.

Movement within the Constant Domain Is Restricted to the A-B Loop

To establish the extent of conformational change within the C domain of the TCR upon Ag ligation, six additional single-site cysteine substitutions were initially made within the constant domain of the LC13 TCR, labeled with NBD, and assayed for changes in fluorescence upon HLA-$B8^{FLR}$ binding (Figure 1E; Table 1). Two of these residues in the A-B loop, Ser131α and Ser134α (Figures 1C and 1D), exhibited a change in fluorescence intensity upon HLA-$B8^{FLR}$ ligation of approximately 15% and 10%, respectively, and these changes were observed in multiple experiments. Importantly, we determined the apparent equilibrium affinity constant of the proposed conformational change for $LC13^{S131C\text{-}NBD}$ and $LC13^{S134C\text{-}NBD}$ to be 6.88 ± 1.99 μM and 1.56 ± 0.40 μM, respectively (Figures 3A and 3B; Table 1). This correlates well with the value obtained for $LC13^{S133C\text{-}NBD}$. Other positions within the constant domain that were tested for movement were the F-G loop (Arg230β) and residues within the Cβ strand-A (Glu127β and Ala129β) and strand-G (Ser239β) (Figure 1E). These sites were tested because they had previously been proposed to represent a docking site for CD3εγ (Sun et al., 2001). There was no change in the fluorescence intensity spectra of $LC13^{R230C\text{-}NBD}$, $LC13^{A129C\text{-}NBD}$, $LC13^{E127C\text{-}NBD}$, or $LC13^{S239C\text{-}NBD}$ (Figure 3A) in the presence of saturating concentration of HLA-$B8^{FLR}$. We then extended this analysis to three additional single-site cysteine substitutions, namely at sites Ser170 (α chain, D-E loop), Ser151 (α chain, C strand), and Ser139 (β-chain, A-B loop) in the LC13 TCR (Figure 1E). These sites were chosen because they represented candidate CD3 binding sites (Kuhns and Davis, 2007) and were also located within potentially flexible regions of the C domain of the TCR (Kjer-Nielsen et al., 2002b). There was no change in the fluorescence intensity spectra of $LC13^{S170C\text{-}NBD}$, $LC13^{S151C\text{-}NBD}$, and $LC13^{S139C\beta\text{-}NBD}$ (Figure 3A) in the presence of saturating concentration of HLA-$B8^{FLR}$. These observations are consistent with the Ag-induced conformational change being restricted to the A-B loop of the Cα domain.

The A-B Loop Movement Is Reversible

If the A-B loop of the TCR acts as a dynamic switch upon Ag ligation, then an important consideration is reversibility of the conformational change upon removal of the Ag stimulation. Hence, if the interaction between $LC13^{S133C\text{-}NBD}$-HLA-$B8^{FLR}$ is disrupted, such as in a competition assay with wild-type recombinant LC13 TCR, the conformation of A-B loop should return, as judged by fluorescence measurements, to its original, nonliganded state. As demonstrated, there is an approximately 20% change in fluorescence intensity in the emission spectrum of $LC13^{S133C\text{-}NBD}$ when a saturating concentration of HLA-$B8^{FLR}$ is added (Figure 3C). Upon adding 23 μM of unlabelled LC13 to the $LC13^{S133C\text{-}NBD}$-HLA-$B8^{FLR}$ sample, the fluorescence intensity decreased to less than 5%, which was similar to the unliganded $LC13^{S133C\text{-}NBD}$ emission spectrum (Figure 3C). The apparent equilibrium Kd of this "reverse interaction" was 6.97 ± 1.75 μM, which is similar to affinity determined for the Ag-induced movement of the A-B loop (Figure 3D; Table 1). Accordingly, these observations show that the movement of the A-B loop is reversible and is dictated by Ag ligation.

Inhibition of the A-B Loop Conformational Change

There are two potential pathways, which are not mutually exclusive, that would enable pMHC-ligation at the Ag binding site to be propagated distally to a conformational change in the A-B loop of the TCR. First, given that the A-B loop is a continuation of the CDR3α loop, conformational changes in the CDR3α loop upon Ag ligation could be transmitted to the A-B loop where they could impact on CD3 conformation (see Movie S1 in which the crystal structure of the nonligated and ligated LC13 TCR is compared). Second, a number of structural studies have shown that there is a change in the juxtapositioning of the Vα-Vβ domains upon Ag ligation and that such changes could be propagated to the constant domain of the TCR, and indeed a recent report has further highlighted this possibility (Ishizuka et al., 2008). Definitively tracking such conformational changes can be problematic, however, because the structures that are determined represent the static end-points, and as such we generally lose any concept of the dynamics of this interaction, and thus the established technology for mapping the pathway of conformational change is not yet established. Nevertheless, to establish

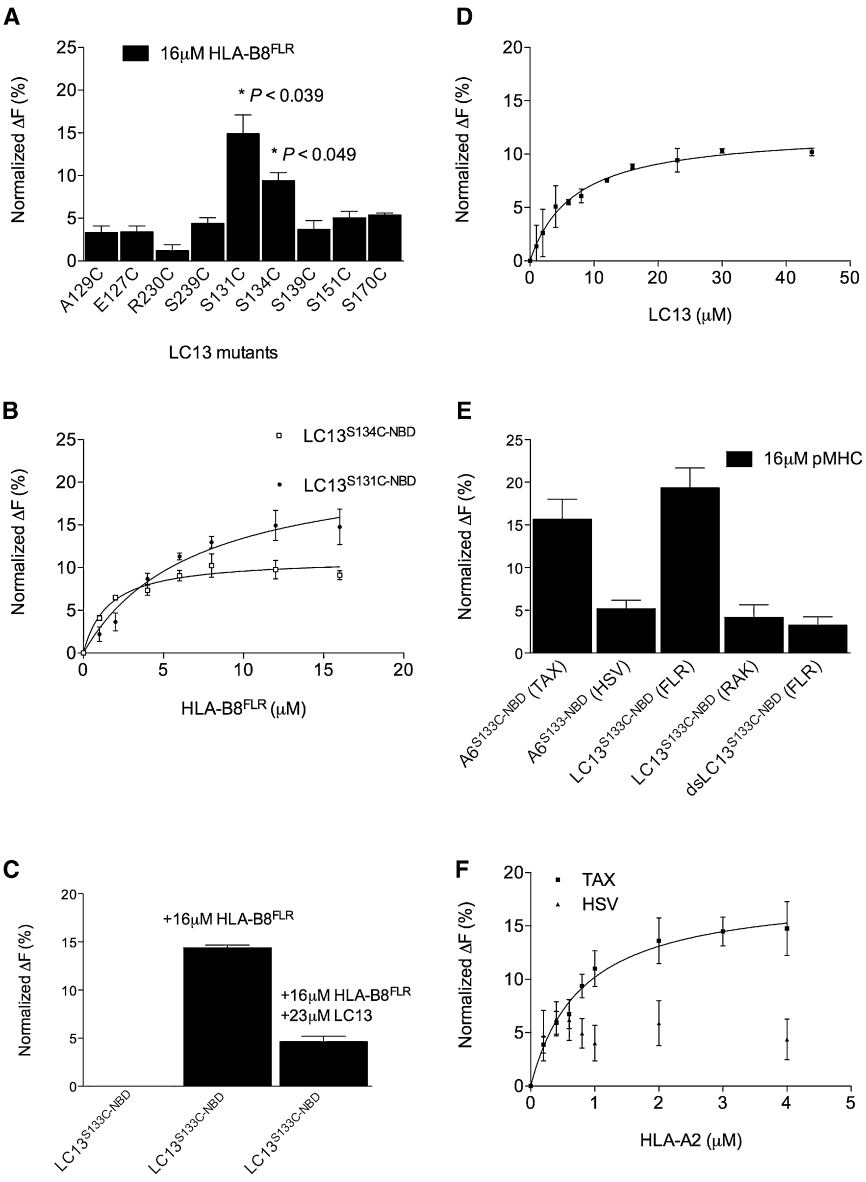

Figure 3. A-B Loop Movement Is Reversible and Generic to Other TCRs

(A) The change in emission intensity of NBD at different positions in LC13 in the presence of 16 μM HLA-B8^{FLR}.

(B) The change of fluorescence intensity of LC13$^{S131C-NBD}$ and LC13$^{S134C-NBD}$ was fitted to a single-site model.

(C and D) The change in fluorescence intensity when LC13$^{S133C-NBD}$ is saturated with HLA-B8^{FLR}. This fluorescence intensity was decreased by titrating increasing concentrations of unlabelled LC13. The percentage change of fluorescence intensity LC13$^{S131C-NBD}$ + HLA-B8^{FLR} + LC13 was fitted to a single-site model.

(E) The percentage change of fluorescence emission spectra of dsLC13$^{S133C-NBD}$ in the presence of 16 μM HLA-B8^{FLR} (n = 3) and A6$^{S133C-NBD}$ in the presence of 4 μM HLA-A2^{TAX} (n = 2) or HLA-A2^{HSV} (n = 3) (the control peptide from herpes simplex virus, VLVDAIVRVA).

(F) The change of fluorescence of A6 was fitted to a single-site binding model (solid line).

whether a conformational change was propagated from the V domains to the C domains upon Ag ligation, we utilized a system where a disulfide bond is introduced between the Cα and Cβ domains of the TCR (dsTCR), which has been shown to stabilize TCRs without changing the affinity of TCRs for Ag (Boulter et al., 2003). The dsLC13^{S133C} was refolded and shown to contain the engineered intermolecular disulfide bond (data not shown), to exhibit identical chromatographic properties as LC13^{S133C}, and to be able to bind HLA-B8^{FLR} with identical affinity to that of the LC13 TCR-HLA-B8^{FLR} interaction (data not shown). There was minimal change in fluorescence intensity (<5%) when the NBD-labeled TCR (dsLC13$^{S133C-NBD}$) was incubated with HLA-B8^{FLR} (Figure 3E), suggesting that the intermolecular disulfide bond between the constant domains inhibited conformational movement of the A-B loop. This is consistent with the observations that Ag ligation propagates a signal from the V domains to the C domains.

Movement of the A-B Loop in Another TCR

In addition to the crystallographic evidence pointing toward the generality of movement in the A-B loop in other TCRs upon Ag ligation, we examined another TCR-pMHC system by using fluorescence-based experiments to further assess the dynamic conformational change of this loop. The HLA-A2-restricted A6 TCR was chosen for investigation because it did not require an engineered disulfide bond between the C domains for refolding, and furthermore, the A6 TCR, and its interaction with HLA-A2 bound to the TAX peptide (HLA-A2^{TAX}), has been characterized extensively at the structural and biophysical level (Ding et al., 1998; Garboczi et al., 1996). Via the same approach for the LC13 system, incubation of HLA-A2^{TAX} against A6$^{S133C-NBD}$ resulted in a 15% change in fluorescence intensity of the probe (Figure 3E), whose apparent equilibrium affinity constant for conformational change in the A-B loop matched that of the affinity constant for Ag ligation (Kd ≈ 1 μM) (Figure 3F; Ding et al., 1998). Importantly, the A-B loop did not change conformation when A6$^{S133C-NBD}$ was incubated with an irrelevant HLA-A2-restricted peptide (Figures 3E and 3F). This indicated that movement in the A-B loop upon Ag ligation is not a property of a single TCR and is a property that is potentially applicable to other TCRs.

Agonist versus Antagonist Recognition

Altered peptide ligands (APLs) can have markedly different signaling outcomes compared to the authentic agonist ligand, yet studies reported that there are few structural differences at the TCR-pMHC interface when ligated to various APLs (Rudolph

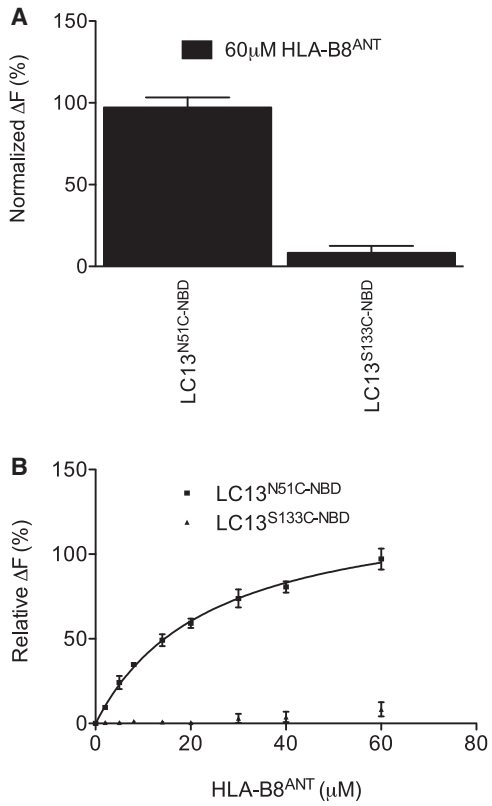

Figure 4. The Interaction of Antagonist Ligand with LC13 Causes No Movement in A-B Loop

(A) The percentage change of fluorescence intensity of $LC13^{N51C\text{-}NBD}$ and $LC13^{S133C\text{-}NBD}$ at 60 μM $HLA\text{-}B8^{ANT}$.

(B) The change of fluorescence intensity at 535 nm for $LC13^{N51C\text{-}NBD}$ and $LC13^{S133C\text{-}NBD}$ is plotted against concentration of $HLA\text{-}B8^{ANT}$ and fitted to a single-site model.

et al., 2006). We reasoned that one potential difference in these divergent signaling outcomes might reside in the differential ability of the agonist or antagonist to trigger a conformational change in the A-B loop. Indeed, close examination of the A6 TCR-HLA A2-APL structural studies indicates that the conformations of the A-B loop in the antagonist or weak agonist complexes are consistent with the "closed" conformation (see Supplemental Data; Ding et al., 1998, 1999). Recently, an APL, FLRGRFGYL ($HLA\text{-}B8^{ANT}$), has been described (Ely et al., 2005) that acts as an antagonist for the LC13-$HLA\text{-}B8^{FLR}$ interaction. The LC13-$HLA\text{-}B8^{ANT}$ interaction is of much weaker affinity compared to the cognate interaction (Kd ≈ 10 μM), and so we aimed to establish whether the LC13-$HLA\text{-}B8^{ANT}$ interaction led to a conformational change in the A-B loop. First, by using the $LC13^{N51C\text{-}NBD}$, we determined the affinity of the interaction with $HLA\text{-}B8^{ANT}$. The $LC13^{N51C\text{-}NBD}$ exhibited increase in intensity when increasing concentrations of $HLA\text{-}B8^{ANT}$ was added (data not shown). This behavior was identical to that observed in the $LC13^{N51C\text{-}NBD}$-$HLA\text{-}B8^{FLR}$ interaction (Figure 2B), suggesting that the interaction between $LC13^{N51C\text{-}NBD}$-$HLA\text{-}B8^{ANT}$ is being monitored correctly. The affinity of this interaction as calculated by the change of fluorescence was 24.09 ± 2.88 μM (Figure 4B). When the same concentration range of $HLA\text{-}B8^{ANT}$ was titrated against $LC13^{S133C\text{-}NBD}$, there was no change in fluorescence intensity at the wavelength maximum of 535 nm (Figures 4A and 4B). These results indicate that the cognate ligand and the antagonist ligand have a differential ability to change the conformation of the A-B loop.

Impact of Mutations within the A-B Loop

The movement in the A-B loop of Cα is coincident with antigen-specific TCR ligation, making it a possible candidate for sensing antigen recognition and transmitting this to CD3. Therefore, we introduced a number of mutations into the residues comprising the A-B loop, and other regions of the constant domain, and tested their impact on T cell activation in a cell-based system. A CD8αβ construct was first stably expressed by retroviral gene transduction into the TCR-negative, human T cell line Jurkat. The $CD8^+$ Jurkat cells were then individually transduced with retroviral expression constructs encoding the LC13 TCR cDNA with the wild-type A-B loop ^{130}DSKSSDK^{136} (*AB-Wt*); deletion of the A-B loop residues SKSSDK (*AB-Del*); charge reversals resulting in the A-B loop sequence DEEEEDK (*AB-Rev*); lengthening of the A-B loop to contain the residues DSKAAAAAAAASSDK (*AB-Len*); alanine substitution of the A-B loop from the wild-type DSKSSDK to AAAAAAA (*AB-Ala*); with potential disulfide bonding of the TCR constant domains by introducing cysteine substitutions at Cys-α (Thr178Cys) and Cys-β (Ser189Cys) (*αβ-Cys*); and alanine substitution of the wild-type residues MRSMDF to MAAAAF in the D-E loop of Cα, previously documented to impair TCR-mediated T cell activation (*DE-Ala*) (Kuhns and Davis, 2007). It was evident from the polyclonal transformants that expression of the LC13 TCR was relatively inefficient for the receptors containing the A-B loop deletion and charge reversal mutations (not shown), highlighting the challenge in understanding the precise relationship between CD3-TCR coexpression on the cell surface and mechanisms underpinning TCR-CD3 triggering via a mutagenesis approach. Nonetheless, after three rounds of cloning, $CD8^+$ Jurkat T cells expressing wild-type and mutant LC13 TCRs were closely matched for levels of TCR expression as judged by staining with $HLA\text{-}B8^{FLR}$ tetramers (Figure 5A). Antigen-specific activation of the Jurkat transformants was assayed by the upregulation of cell surface CD69 2 hr after incubation with graded concentrations of $HLA\text{-}B8^{FLR}$ tetramers. As shown in Figure 5B, the dose dependence and maximal degree of CD69 upregulation varied among the transduced cells, with wild-type LC13 Jurkat cells showing the most efficient stimulation. As expected, Jurkat cells expressing the DE-Ala mutant showed a dose-dependent reduction in their T cell activation, whereas the LC13 TCR receptors with engineered Cys residues in their constant domains also demonstrated reduced activation. Although activation of the αβ-Cys mutant was only partially inhibited, this is consistent with the impaired change in ligand-induced fluorescence intensity of the $dsLC13^{S133C}$ recombinant TCR containing the engineered intermolecular disulfide bond introduced between the Cα and Cβ domains of the TCR. Although we cannot confirm the efficiency of the engineered intermolecular disulfide bond in the Jurkat-expressed LC13 TCR, the findings suggest that this bond does form naturally in the cell-based system potentially linking A-B loop movement with reduced TCR signaling. The AB-Del, AB-Rev, AB-Len, and AB-Ala loop mutations in LC13 TCR

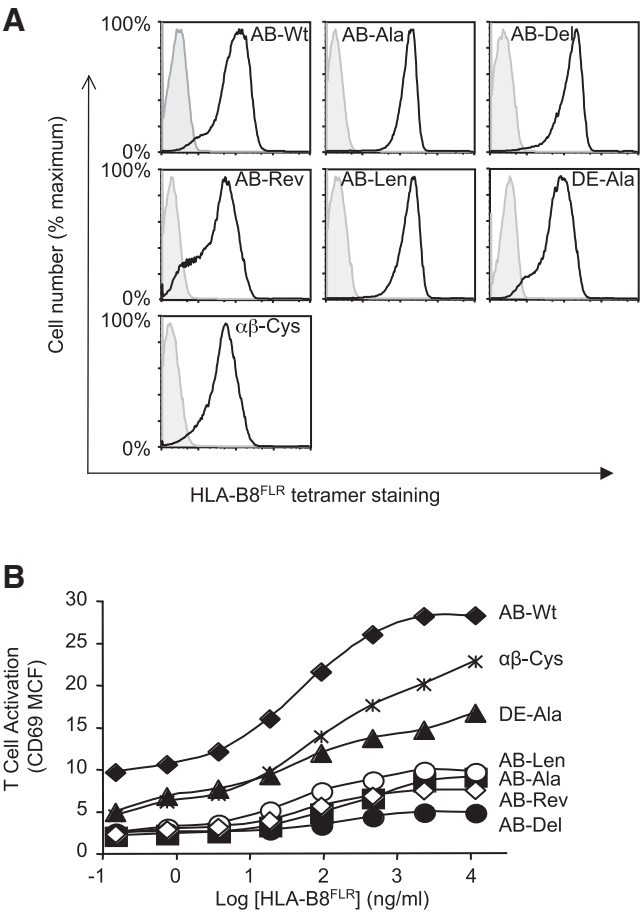

Figure 5. Functional Evidence that the Movement in the A-B Loop of the TCR Cα Domain Is Involved in Early TCR Signaling

(A) Surface expression of wild-type and mutant LC13 TCR molecules on retrovirally transduced Jurkat cells. $CD8^+$ Jurkat cells were individually transduced with retroviral expression constructs encoding the LC13 TCR cDNA containing the wild-type A-B loop (AB-Wt); a deletion of the A-B loop residues SKSSDK (AB-Del); charge reversals resulting in the A-B loop sequence DEEEEDK (AB-Rev); lengthening of the A-B loop to contain the residues DSKAAAAA AAASSDK (AB-Len); alanine substitution of the A-B loop from the wild-type DSKSSDK to AAAAAAA (AB-Ala); cysteine substitutions at Cys-α (T178C) and Cys-β (S189C) (αβ-Cys) to engender potential disulfide bonding of the TCR constant domains; and a polyalanine substitution of the wild-type residues MRSMDF to MAAAAF in the D-E loop of Cα (DE-Ala), previously documented to impair TCR-mediated T cell activation (Kuhns and Davis, 2007). Three successive rounds of cloning the $CD8^+$ Jurkat T cells expressing wild-type and mutant LC13 TCRs were necessary to match transformants as closely as possible for levels of TCR expression. Cells were stained with HLA-$B8^{FLR}$ tetramer (PE labeled) at room temperature for 45 min and analyzed by FACs. Staining with HLA-$B8^{FLR}$ tetramer is shown as a log scale. Shaded histogram indicates background staining of the relevant cells in the absence of tetramer.

(B) Antigen-specific activation of Jurkat T cells transduced with parental LC13 and mutant TCRs described above. Jurkat transformants (2×10^5) were plated in a U-bottom 96-well plate and HLA-$B8^{FLR}$ tetramer (APC labeled) was added to the cells at the indicated final concentration then mixed. After culture at 37°C for 2 hr, the plate was cooled on ice for 5 min and the cells were pelleted at 1200 rpm at 4°C. The cells were stained with CD69 mAb (PE labeled) (30 min on ice) and washed twice, and the mean channel fluorescence (MCF) of CD69 staining was determined by flow cytometry. All Jurkat transformants were activated after stimulation with OKT3 mAb (not shown). The experiment was conducted twice with similar results.

were all associated with markedly impaired upregulation of CD69 after antigen-specific ligation (Figure 5B; Figure S3) despite activation of these cells by stimulation with the CD3 mAb OKT3 (data not shown). Given the nature of the introduced TCR mutations, the reduced T cell activation in the LC13 mutants may also arise from impaired TCR stability or assembly. Therefore it is noteworthy that ligand-induced downregulation of LC13 TCR was observed in all transformants after incubation of Jurkat T cells with HLA-$B8^{FLR}$ tetramers at 37°C (not shown), implying that TCR clustering and internalization still occurred in the mutant TCRs after Ag-specific ligation. Taken together, the data are consistent with ligation-induced movement of the A-B loop playing an important role in the events underpinning early TCR signaling.

DISCUSSION

The mechanism by which receptor-ligand ligation results in a signal being transmitted within the cell remains a key question in a number of distinct biological systems. In the context of T cell signaling, this extracellular-intracellular communication event is even more intriguing because the TCR does not possess signaling domains themselves; accordingly, pMHC ligation has to be communicated to the CD3 signaling apparatus to which the TCR is noncovalently associated. Our structural and SDFL data demonstrate that Ag ligation leads to a discrete conformational change within the A-B loop of the constant domain of the LC13 TCR, and this conformational change is MHC restricted and coincident with that of Ag ligation, and is reversible upon disengagement of the TCR. The conformational change in the A-B loop of the TCR upon pMHC ligation although clearly evident is also subtle and this is reflected in the changes in fluorescence caused by Ag ligation. The fluorescence-based measurements reported here are highly reproducible and statistically significant, generate a dose-dependant response, and are well within the range of other conformational changes measured with NBD as a probe (Gether et al., 1997; Gibson et al., 1997; Jensen et al., 2001). We have also observed this A-B loop conformational change in two distinct, well-described TCR systems (namely the LC13 and A6 TCR), and it will be important to test the further generalities of these findings in other TCR systems, including that of murine TCRs. Accordingly, at this stage it is unclear whether all TCRs have a propensity for a similar conformational change within the constant domain of the TCR, or whether it represents a property of certain TCRs, such as immunodominant TCRs for example (Ishizuka et al., 2008; Wang et al., 2008), or whether it represents the vestiges of a primordial TCR signaling mechanism.

Accordingly, our data are consistent with a conformational model of T cell triggering mediated by antigen ligation of the αβ TCR. A conformational basis for T cell triggering is in agreement with previous findings, where (1) ligation by TCR and CD3 mAbs, monovalent Fab fragments, and pMHC ligands led to a conformational change within the CD3ε cytoplasmic domain (Gil et al., 2002, 2005; Minguet et al., 2007; Risueno et al., 2005) and in addition the conformation of the CD3ζζ chains are considered to be contingent on their immediate environment (Aivazian and Stern, 2000); (2) T cell signaling occurs before the formation of the immunological synapse and that a single pMHC agonist is

sufficient to initiate T cell signaling, which suggests that T cell triggering must be intrinsic to the CD3-TCR-pMHC interaction; (3) furthermore, thermodynamic considerations indicated that TCR-pMHC engagement induced a torque within the TCR (Krogsgaard et al., 2003). Although studies have shown that clustering of TCR-CD3 complexes play a role in T cell signaling, our data reveal that conformational change within the constant domain is independent of TCR dimerization, but it can nevertheless potentially promote TCR dimerization. It is possible that clustering reflects a later evolutionary addition that serves to amplify initial signaling. Although the precise geometry of the TCR-CD3 complex is unknown and mutagenesis studies have been ambiguous in defining TCR-CD3 interaction sites, the movement of the A-B loop may also permit differential juxtapositioning of the TCR-CD3 complex, thereby leading to a signal being transmitted intracellularly. Ultimately to test this "molecular switch" hypothesis, structural studies of complexes between the TCR and CD3 components will be required to reveal the detailed architecture of this interaction. It will also be useful to undertake double-labeling experiments of the TCR with two distinct fluorochromes so that the time dependence of the increased fluorescence intensity of the A-B loop can be measured with respect to pMHC binding.

Movement within the constant domain was not observed upon binding to an antagonist pMHC ligand, which may permit different signals to propagate intracellularly upon APL engagement, which is consistent with partial agonists and antagonists being unable to transmit a conformational change to the intracellular domains of CD3ε (Risueno et al., 2005). Moreover, although the conformational changes at the TCR-pMHC interface may be small when comparing cognate and APL complexes, the differing molecular torque that has been observed to exist between various TCR-pMHC complexes may serve as a means to propagate a differing signal to the C domain of the TCR (Krogsgaard et al., 2003). It will be of interest to establish whether other receptors, including the γδ TCR, the pre-Tα receptor, and the B cell receptor, which adopt a similar architecture to that of the αβ TCR, transduce signals in a similar manner shown for the αβ TCR. Regardless, our findings provide a crucial link between TCR ligation and distal conformational adjustments that can potentially impact on the CD3 signaling molecules.

Importantly, lengthening, deleting, or substituting residues in the A-B loop of the LC13 TCR is associated with markedly impaired upregulation of CD69 after antigen-specific stimulation in a T cell-based system. Modest impairment of signaling was also observed in LC13 receptors with engineered Cys residues in their constant domains, potentially forming an intermolecular disulfide bond between the Cα and Cβ domains, thus "fixing" the juxtaposition of the V regions within the TCR. Impairment in signaling was at least comparable to that observed for mutations in the D-E loop of the TCR α chain constant domain, previously reported by others (Kuhns and Davis, 2007) to affect TCR signaling. Collectively, the data provide supporting evidence for the functional role of the A-B loop in the context of T cell triggering. Even so, we are mindful that the A-B loop mutations may also alter aspects of TCR stability and assembly affecting TCR dimerization or TCR-CD3 juxta-positioning.

Our findings suggest a basis for understanding the earliest events in TCR signaling in which antigen recognition by the TCR αβ heterodimer potentially transmits Ag recognition to the CD3 signalosome via a conformational change in the constant domain of the TCR α chain.

EXPERIMENTAL PROCEDURES

Structural Data

For the structural comparisons of the A-B loop conformation, TCR structures, nonliganded and pMHC ligated were downloaded from the PDB (see Table S1). Only the structures of TCRs in which the complete ectodomains (namely variable and constant domains) were analyzed are reported within this table.

Construction of TCR Mutants

The original LC13 TCR clone was prepared as previously described (Kjer-Nielsen et al., 2002b) and used as template to generate the TCR mutants by site-directed mutagenesis (QuikChange; Stratagene, La Jolla, CA).

Expression and Purification of Recombinant Proteins

Soluble HLA-B8^{FLR} and HLA-A2^{TAX} complexes were prepared from *E. coli* as described previously (Garboczi et al., 1992; Kjer-Nielsen et al., 2002a). The refolded complexes were concentrated and purified by anion exchange and gel filtration chromatography. The α and β chains of LC13 TCR were expressed in BL21 (DE3) *E. coli* cells, refolded from inclusion bodies, and purified as previously described (Kjer-Nielsen et al., 2003). The structural integrity of the refolded proteins was confirmed by apparent molecular weight of the protein after size exclusion chromatography and by SDS-PAGE.

Modification of Cysteine-Substituted TCR with IANBD or IAEDANS

In a typical labeling reaction, 0.5 mg of TCR in 10 mM Tris-HCl (pH 7.4), 150 mM NaCl was labeled with 20-fold molar excess of IANBD or IAEDANS (Molecular Probes, Eugene, OR) and incubated at 4°C on rotating wheel for 16 hr. The labeled TCR was separated from free label by passing over a 5 ml Desalting column (GE Healthcare) equilibrated in 10 mM Tris-HCl (pH 8.0), 150 mM NaCl, and 2 mM EDTA. The extent of the covalent reaction was estimated with the extinction coefficient of ε_{478nm} of 25,000 M^{-1} cm^{-1} for NBD and ε_{340nm} of 5,700 M^{-1} cm^{-1} for AEDANS (Haugland, 1996). The labeling procedure resulted in incorporation of between 0.6 to 0.9 mol of NBD or AEDANS per mol of TCR.

Spectrofluorometry Methods

Fluorescence emission spectra were recorded on a PerkinElmer Life Sciences LS50B spectrofluorimeter by using a temperature-controlled cuvette at 25°C in a 1 cm path length quartz cell. Excitation and emission slits were set at 7.0 nm for all spectra, unless otherwise stated, and a scan speed of 10 nm/min was used. Unless otherwise stated, 2 μM NBD-labeled TCR was excited at 478 nm, with fluorescence emission spectra measured from 500 to 600 nm. Each concentration of MHC was added and allowed to mix for 1 min before recording of the spectra. The AEDANS-labeled TCR was excited at 340 nm, with fluorescence emission spectra measured from 400 to 650 nm. All of the samples tested had an absorbance of less than 0.1 at 535 nm in the concentrations used excluding any "inner filter" effect in the fluorescence experiments (data not shown). All changes in fluorescence spectra were corrected for dilution effects. The percentage change in fluorescence was calculated as

$$\%\Delta F = (F_I - F_o)/F_{LC13N51} \quad (1)$$

where F_I is fluorescence intensity at *x* concentration of TCR-pMHC complex, F_O is the initial intenstity of the TCR, and $F_{LC13N51}$ is the maximum fluorescence change at 16 μM HLA-B8^{FLR}. The means of three independent experiments were fitted with Graphpad version 3.0 (GraphPad software).

Generation of CD8$^+$ Jurkat Cells and LC13 Mutants

LC13 αβ TCR cDNA was reverse transcribed from LC13 T cell clone RNA via Superscript II (Invitrogen). LC13α (primers P1 and P2) and β chain (P3 and P4) gene segments were amplified by PCR with the following primers: **P1**: 2A-LC13a-For:(**EcoRI**) 5′- CG**GAATTC**GCTAGCCACCatgaagttggtgacaagc; **P2**: hTRa.F2Agsg-Rev (BamHI, **KasI/NarI**) 5′GGGCCCTGGGTTCTCTTCGAC

GTCGCCGGCCTGCTTAAGCAGCGAGAAATTGGT**GGCGCC**GGATCCgctgg accacagccgcagcgt; **P3**: gsgF2A-LC13b-For (BamHI, **KasI/NarI**) 5′GGATCC **GGCGCC**ACCAATTTCTCGCTGCTTAAGCAGGCCGGCGACGTCGAAGAGA ACCCAGGGCCCatgggcaccaggctcctctgc; **P4**: hTRbetaC2-Rev: (**XhoI**) 5′ CC G**CTCGAG***CTGCAG***cta**gcctctggaatcctttct.

CD8α cDNA was purchased from OriGene. CD8α primers (P5 and P6) and CD8β primers (P7 and P8) were used to generate PCR products encoding the CD8α and β chains: **P5**: CD8aEcoRI-For5′cGAATTCcgtcctggggagcgcgtcat; **P6**: CD8aXhoI-Rev 5′ gCTCGAGcagggttagacgtatctcgc; **P7**: CD8bEcoRI-For 5′cGAATTCggtgtcccgggcgcgccacg; **P8**: CD8bXhoI-Rev 5′gCTCGAGtcgtgctc gttactgaccga.

Amplicons were then cloned into pGEM-T Easy (Promega). These were verified by sequencing, before being transferred separately into the retroviral expression vector pMIG (denoted as pMIG-CD8α and pMIG-CD8β, respectively).

PCR products encoding LC13α and β chains were cloned into pGEM-T Easy prior to cotransfer into the pMIG vector. The LC13α and LC13β gene segments when expressed are predicted to be linked by a self-cleaving 2A peptide (Szymczak et al., 2004), allowing for subsequent surface expression of the LC13 αβ TCR.

All the LC13 mutants were generated from the parental pGEM-LC13α-2A-LC13β (*AB-Wt*) plasmid through site-directed mutagenesis. The four α chain A-B loop mutants included deletion of the A-B loop residues SKSSDK (*AB-Del*); charge reversals resulting in the A-B loop sequence DEEEEDK (*AB-Rev*); lengthening of the A-B loop to contain the residues DSKAAAAAAAASSDK (*AB-Len*); and alanine substitution of the A-B loop from the wild-type DSKSSDK to AAAAAAA (*AB-Ala*). A mutant with potential disulphide bonding of the TCR constant domains was created by introducing cysteine substitutions at Cys-α (T178C) and Cys-β (S189C) (*αβ-Cys*). A positive control signaling mutant contained alanine substitution of the wild-type residues MRSMDF to MAAAAF in the D-E loop of Cα, previously documented to impair TCR-mediated T cell activation (ref) (*DE-Ala*). The mutagenesis primers were as follows: AB-Ala: 5′CCTGCCGTGTACCAGCTGAGAgcagctgcagcagctgctgccTCTGTCTGCCTA TTCACCGAT, resulting in the following A-B loop residues being altered from DSKSSDK (wild-type) to AAAAAAA (mutant). AB-Del: 5′gccgtgtaccagctgagaga cTCTGTCTGCCTATTCACCGAT, resulting in the mutant A-B loop lacking the residues: SKSSDK……; AB-Rev: 5′GCCGTGTACCAGCTGAGAGACgaagagg aagagGACAAGTCTGTCTGCCTATTCACC, resulting in the mutant A-B loop containing the residues DEEEEDK; AB-Len: 5′TACCAGCTGAGAgactctaaa gcagctgcagcagctgctgccgcctccagtgacaagTCTGTCTG, resulting in the mutant A-B loop containing the residues DSKAAAAAAAASSDK; DE-Ala: 5′ACAGACA AAACTGTGCTAGACATGgcagctgcagcaTTCAAGAGCAACAGTGCTGTG, resulting in the D-E loop being altered from MRSMDF (wild-type) to MAAAAF (mutant); αβ-Cys: Cys-α(T178C): GTATATCACAGACAAAtgTGTGCTAGACAT GAGG; Cys-β (S189C): CACAGTGGGGTCtGCACAGACCCGC.

Retroviral-Mediated Gene Transduction into Jurkat Cells

The plasmids pMIG-CD8α (4 μg) and pMIG-CD8β (4 μg) encoding the CD8α and CD8β chains were individually combined with the packaging vectors pPAM-E (4 μg) and pVSV-g (2 μg) and transfected into 10^6 293T cells in a 10 cm dish as previously described with Fugene 6 (Roche) (Holst et al., 2006). The transiently transfected 293T cells were further cultured for 5 days. During this time, the retrovirus-containing supernatant was collected twice daily, combined, and used to transduce Jurkat (3T3.5) cells along with polybrene (6 μg/ml). At the end of the transduction, Jurkat cells were analyzed for expression of GFP and CD8αβ (CD8β-PE staining) by fluorescence-activated cell sorting. Jurkat.CD8αβ-positive cells were enriched by cell sorting and were subsequently cloned by single-cell sorting by flow cytometry.

Similarly, the wild-type and mutant pMIG-LC13αβ DNAs were individually combined with the packaging vectors pPAM-E and pVSV-g and transfected into 293T cells separately. The supernatant from each transfection was applied to Jrt.CD8αβ cells along with polybrene. After fluorescence-activated cell sorting and single cell cloning, 7 cell clones were thus generated: Jrt.CD8αβ.LC13wt (AB-Wt), Jrt.CD8αβ.LC13Scan (AB-Ala), Jrt.CD8αβ.LC13Del (AB-Del), Jrt.CD8αβ.LC13DEscan (DE-Ala), Jrt.CD8αβ.LC13CR (AB-Rev), Jrt.CD8αβ.LC13Len (AB-Len), and Jrt.CD8αβ.LC13Cys (αβ-Cys).

T Cell Activation Assays

2×10^5 Jrt.CD8αβ.LC13 cells were cultured with or without antigen stimulation for 2 hr at 37°C. The antigen stimulation was carried out with HLA-B8 tetramers loaded with the FLRGRAYGL (FLR) peptide from Epstein Barr virus EBNA3A. Control T cell stimulation was carried out with the CD3 mAb, OKT3. After incubation with free ligand, the responder cells were pelleted and assayed for CD69 upregulation by staining and visualization by a fluorescence-activated cell sorter. T cell activation was measured by the increase in the mean channel fluorescence (MCF) of CD69-stained Jurkat transformants.

SUPPLEMENTAL DATA

Supplemental Data include one figure, one table, and one movie and can be found with this article online at http://www.cell.com/immunity/supplemental/S1074-7613(09)00195-2.

ACKNOWLEDGMENTS

We thank N. La Gruta and R. Tweten for useful discussions and D. Garboczi for the generous provision of the A6 TCR plasmids. The Australian Research Council (ARC), the National Health and Medical Research Council of Australia (NHMRC), the Roche Organ Transplantation Research Fund, Monash University Strategic grant, and ANZ trustees supported this research. T.B. is an NHMRC CDA fellow; W.A.M. and M.A.D. are supported by NHMRC Peter Doherty Fellowships; L.K.E. is supported by a NHMRC CJ Martin Fellowship; M.C.J.W., S.R. Burrows, and S.P.B. are supported by a NHMRC Senior Research Fellowship; C.S.C. is supported by an ARC QEII fellowship; and J.R. is supported by an ARC Federation Fellowship.

Received: December 14, 2007
Revised: February 16, 2009
Accepted: March 17, 2009
Published online: May 21, 2009

REFERENCES

Aivazian, D., and Stern, L.J. (2000). Phosphorylation of T cell receptor zeta is regulated by a lipid dependent folding transition. Nat. Struct. Biol. *7*, 1023–1026.

Alarcon, B., Swamy, M., van Santen, H.M., and Schamel, W.W. (2006). T-cell antigen-receptor stoichiometry: pre-clustering for sensitivity. EMBO Rep. *7*, 490–495.

Arnett, K.L., Harrison, S.C., and Wiley, D.C. (2004). Crystal structure of a human CD3-epsilon/delta dimer in complex with a UCHT1 single-chain antibody fragment. Proc. Natl. Acad. Sci. USA *101*, 16268–16273.

Baker, B.M., and Wiley, D.C. (2001). [alpha][beta] T cell receptor ligand-specific oligomerization revisited. Immunity *14*, 681–692.

Borg, N.A., Ely, L.K., Beddoe, T., Macdonald, W.A., Reid, H.H., Clements, C.S., Purcell, A.W., Kjer-Nielsen, L., Miles, J.J., Burrows, S.R., et al. (2005). The CDR3 regions of an immunodominant T cell receptor dictate the 'energetic landscape' of peptide-MHC recognition. Nat. Immunol. *6*, 171–180.

Borg, N.A., Wun, K.S., Kjer-Nielsen, L., Wilce, M.C., Pellicci, D.G., Koh, R., Besra, G.S., Bharadwaj, M., Godfrey, D.I., McCluskey, J., and Rossjohn, J. (2007). CD1d-lipid-antigen recognition by the semi-invariant NKT T-cell receptor. Nature *448*, 44–49.

Boulter, J.M., Glick, M., Todorov, P.T., Baston, E., Sami, M., Rizkallah, P., and Jakobsen, B.K. (2003). Stable, soluble T-cell receptor molecules for crystallization and therapeutics. Protein Eng. *16*, 707–711.

Call, M.E., and Wucherpfennig, K.W. (2004). Molecular mechanisms for the assembly of the T cell receptor-CD3 complex. Mol. Immunol. *40*, 1295–1305.

Call, M.E., and Wucherpfennig, K.W. (2005). The T cell receptor: Critical role of the membrane environment in receptor assembly and function. Annu. Rev. Immunol. *23*, 101–125.

Call, M.E., Pyrdol, J., and Wucherpfennig, K.W. (2004). Stoichiometry of the T-cell receptor-CD3 complex and key intermediates assembled in the endoplasmic reticulum. EMBO J. *23*, 2348–2357.

Choudhuri, K., Kearney, A., Bakker, T.R., and van der Merwe, P.A. (2005). Immunology: How do T cells recognize antigen? Curr. Biol. *15*, R382–R385.

Clements, C.S., Dunstone, M.A., Macdonald, W.A., McCluskey, J., and Rossjohn, J. (2006). Specificity on a knife-edge: The alphabeta T cell receptor. Curr. Opin. Struct. Biol. *16*, 787–795.

Cohen, B.E., Pralle, A., Yao, X., Swaminath, G., Gandhi, C.S., Jan, Y.N., Kobilka, B.K., Isacoff, E.Y., and Jan, L.Y. (2005). A fluorescent probe designed for studying protein conformational change. Proc. Natl. Acad. Sci. USA *102*, 965–970.

Crowley, K.S., Liao, S., Worrell, V.E., Reinhart, G.D., and Johnson, A.E. (1994). Secretory proteins move through the endoplasmic reticulum membrane via an aqueous, gated pore. Cell *78*, 461–471.

Deng, L., Langley, R.J., Brown, P.H., Xu, G., Teng, L., Wang, Q., Gonzales, M.I., Callender, G.G., Nishimura, M.I., Topalian, S.L., and Mariuzza, R.A. (2007). Structural basis for the recognition of mutant self by a tumor-specific, MHC class II-restricted T cell receptor. Nat. Immunol. *8*, 398–408.

Ding, Y.H., Smith, K.J., Garboczi, D.N., Utz, U., Biddison, W.E., and Wiley, D.C. (1998). Two human T cell receptors bind in a similar diagonal mode to the HLA-A2/Tax peptide complex using different TCR amino acids. Immunity *8*, 403–411.

Ding, Y.H., Baker, B.M., Garboczi, D.N., Biddison, W.E., and Wiley, D.C. (1999). Four A6-TCR/peptide/HLA-A2 structures that generate very different T cell signals are nearly identical. Immunity *11*, 45–56.

Ely, L.K., Green, K.J., Beddoe, T., Clements, C.S., Miles, J.J., Bottomley, S.P., Zernich, D., Kjer-Nielsen, L., Purcell, A.W., McCluskey, J., et al. (2005). Antagonism of antiviral and allogeneic activity of a human public CTL clonotype by a single altered peptide ligand: implications for allograft rejection. J. Immunol. *174*, 5593–5601.

Ely, L.K., Beddoe, T., Clements, C.S., Matthews, J.M., Purcell, A.W., Kjer-Nielsen, L., McCluskey, J., and Rossjohn, J. (2006). Disparate thermodynamics governing T cell receptor-MHC-I interactions implicate extrinsic factors in guiding MHC restriction. Proc. Natl. Acad. Sci. USA *103*, 6641–6646.

Feng, D., Bond, C.J., Ely, L.K., Maynard, J., and Garcia, K.C. (2007). Structural evidence for a germline-encoded T cell receptor-major histocompatibility complex interaction 'codon'. Nat. Immunol. *8*, 975–983.

Garboczi, D.N., Hung, D.T., and Wiley, D.C. (1992). HLA-A2-peptide complexes: Refolding and crystallization of molecules expressed in *Escherichia coli* and complexed with single antigenic peptides. Proc. Natl. Acad. Sci. USA *89*, 3429–3433.

Garboczi, D.N., Utz, U., Ghosh, P., Seth, A., Kim, J., VanTienhoven, E.A., Biddison, W.E., and Wiley, D.C. (1996). Assembly, specific binding, and crystallization of a human TCR-alphabeta with an antigenic Tax peptide from human T lymphotropic virus type 1 and the class I MHC molecule HLA-A2. J. Immunol. *157*, 5403–5410.

Gether, U., Lin, S., Ghanouni, P., Ballesteros, J.A., Weinstein, H., and Kobilka, B.K. (1997). Agonists induce conformational changes in transmembrane domains III and VI of the beta2 adrenoceptor. EMBO J. *16*, 6737–6747.

Ghendler, Y., Smolyar, A., Chang, H.C., and Reinherz, E.L. (1998). One of the CD3epsilon subunits within a T cell receptor complex lies in close proximity to the Cbeta FG loop. J. Exp. Med. *187*, 1529–1536.

Gibson, A., Baburaj, K., Day, D.E., Verhamme, I., Shore, J.D., and Peterson, C.B. (1997). The use of fluorescent probes to characterize conformational changes in the interaction between vitronectin and plasminogen activator inhibitor-1. J. Biol. Chem. *272*, 5112–5121.

Gil, D., Schamel, W.W., Montoya, M., Sanchez-Madrid, F., and Alarcon, B. (2002). Recruitment of Nck by CD3 epsilon reveals a ligand-induced conformational change essential for T cell receptor signaling and synapse formation. Cell *109*, 901–912.

Gil, D., Schrum, A.G., Alarcon, B., and Palmer, E. (2005). T cell receptor engagement by peptide-MHC ligands induces a conformational change in the CD3 complex of thymocytes. J. Exp. Med. *201*, 517–522.

Godfrey, D.I., Rossjohn, J., and McCluskey, J. (2008). The fidelity, occasional promiscuity, and versatility of T cell receptor recognition. Immunity *28*, 304–314.

Gras, S., Kjer-Nielsen, L., Burrows, S.R., McCluskey, J., and Rossjohn, J. (2008). T-cell receptor bias and immunity. Curr. Opin. Immunol. *20*, 119–125.

Haugland, R.P. (1996). Handbook of Fluorescent Probes and Research Chemicals, Sixth Edition (Eugene, OR: Molecular Probes, Inc).

Hayes, S.M., and Love, P.E. (2006). Stoichiometry of the murine gammadelta T cell receptor. J. Exp. Med. *203*, 47–52.

Holst, J., Szymczak-Workman, A.L., Vignali, K.M., Burton, A.R., Workman, C.J., and Vignali, D.A. (2006). Generation of T-cell receptor retrogenic mice. Nat. Protocols *1*, 406–417.

Ishizuka, J., Stewart-Jones, G.B.E., van der Merwe, A., Bell, J.I., McMichael, A.J., and Jones, E.Y. (2008). The structural dynamics and energetics of an immunodominant T cell receptor are programmed by its V[beta] domain. Immunity *28*, 171–182.

Jensen, A.D., Guarnieri, F., Rasmussen, S.G., Asmar, F., Ballesteros, J.A., and Gether, U. (2001). Agonist-induced conformational changes at the cytoplasmic side of transmembrane segment 6 in the beta 2 adrenergic receptor mapped by site-selective fluorescent labeling. J. Biol. Chem. *276*, 9279–9290.

Johnson, A.E. (2005). Fluorescence approaches for determining protein conformations, interactions and mechanisms at membranes. Traffic *6*, 1078–1092.

Kane, L.P., Lin, J., and Weiss, A. (2000). Signal transduction by the TCR for antigen. Curr. Opin. Immunol. *12*, 242–249.

Kjer-Nielsen, L., Clements, C.S., Brooks, A.G., Purcell, A.W., Fontes, M.R., McCluskey, J., and Rossjohn, J. (2002a). The structure of HLA-B8 complexed to an immunodominant viral determinant: peptide-induced conformational changes and a mode of MHC class I dimerization. J. Immunol. *169*, 5153–5160.

Kjer-Nielsen, L., Clements, C.S., Brooks, A.G., Purcell, A.W., McCluskey, J., and Rossjohn, J. (2002b). The 1.5 A crystal structure of a highly selected antiviral T cell receptor provides evidence for a structural basis of immunodominance. Structure *10*, 1521–1532.

Kjer-Nielsen, L., Clements, C.S., Purcell, A.W., Brooks, A.G., Whisstock, J.C., Burrows, S.R., McCluskey, J., and Rossjohn, J. (2003). A structural basis for the selection of dominant alphabeta T cell receptors in antiviral immunity. Immunity *18*, 53–64.

Kjer-Nielsen, L., Dunstone, M.A., Kostenko, L., Ely, L.K., Beddoe, T., Mifsud, N.A., Purcell, A.W., Brooks, A.G., McCluskey, J., and Rossjohn, J. (2004). Crystal structure of the human T cell receptor CD3 epsilon gamma heterodimer complexed to the therapeutic mAb OKT3. Proc. Natl. Acad. Sci. USA *101*, 7675–7680.

Kobilka, B.K., and Gether, U. (2002). Use of fluorescence spectroscopy to study conformational changes in the beta 2-adrenoceptor. Methods Enzymol. *343*, 170–182.

Krogsgaard, M., Prado, N., Adams, E.J., He, X.L., Chow, D.C., Wilson, D.B., Garcia, K.C., and Davis, M.M. (2003). Evidence that structural rearrangements and/or flexibility during TCR binding can contribute to T cell activation. Mol. Cell *12*, 1367–1378.

Kuhns, M.S., and Davis, M.M. (2007). Disruption of extracellular interactions impairs T cell receptor-CD3 complex stability and signaling. Immunity *26*, 357–369.

Mingueneau, M., Sansoni, A., Gregoire, C., Roncagalli, R., Aguado, E., Weiss, A., Malissen, M., and Malissen, B. (2008). The proline-rich sequence of CD3[epsi] controls T cell antigen receptor expression on and signaling potency in preselection CD4+CD8+ thymocytes. Nat. Immunol. *9*, 522–532.

Minguet, S., Swamy, M., Alarcon, B., Luescher, I.F., and Schamel, W.W. (2007). Full activation of the T cell receptor requires both clustering and conformational changes at CD3. Immunity *26*, 43–54.

Risueno, R.M., Gil, D., Fernandez, E., Sanchez-Madrid, F., and Alarcon, B. (2005). Ligand-induced conformational change in the T-cell receptor associated with productive immune synapses. Blood *106*, 601–608.

Rudolph, M.G., Stanfield, R.L., and Wilson, I.A. (2006). How TCRs bind MHCs, peptides, and coreceptors. Annu. Rev. Immunol. *24*, 419–466.

Schamel, W.W., Arechaga, I., Risueno, R.M., van Santen, H.M., Cabezas, P., Risco, C., Valpuesta, J.M., and Alarcon, B. (2005). Coexistence of multivalent and monovalent TCRs explains high sensitivity and wide range of response. J. Exp. Med. *202*, 493–503.

Shatursky, O., Heuck, A.P., Shepard, L.A., Rossjohn, J., Parker, M.W., Johnson, A.E., and Tweten, R.K. (1999). The mechanism of membrane insertion for a cholesterol-dependent cytolysin: a novel paradigm for pore-forming toxins. Cell *99*, 293–299.

Shepard, L.A., Heuck, A.P., Hamman, B.D., Rossjohn, J., Parker, M.W., Ryan, K.R., Johnson, A.E., and Tweten, R.K. (1998). Identification of a membrane-spanning domain of the thiol-activated pore-forming toxin *Clostridium perfringens* perfringolysin O: An α-helical to beta-sheet transition identified by fluorescence spectroscopy. Biochemistry *37*, 14563–14574.

Sun, Z.J., Kim, K.S., Wagner, G., and Reinherz, E.L. (2001). Mechanisms contributing to T cell receptor signaling and assembly revealed by the solution structure of an ectodomain fragment of the CD3 epsilon gamma heterodimer. Cell *105*, 913–923.

Sun, Z.Y., Kim, S.T., Kim, I.C., Fahmy, A., Reinherz, E.L., and Wagner, G. (2004). Solution structure of the CD3epsilondelta ectodomain and comparison with CD3epsilongamma as a basis for modeling T cell receptor topology and signaling. Proc. Natl. Acad. Sci. USA *101*, 16867–16872.

Szymczak, A.L., Workman, C.J., Wang, Y., Vignali, K.M., Dilioglou, S., Vanin, E.F., and Vignali, D.A.A. (2004). Correction of multi-gene deficiency in vivo using a single 'self-cleaving' 2A peptide-based retroviral vector. Nat. Biotechnol. *22*, 589–594.

Turner, S.J., Doherty, P.C., McCluskey, J., and Rossjohn, J. (2006). Structural determinants of T-cell receptor bias in immunity. Nat. Rev. Immunol. *6*, 883–894.

Tynan, F.E., Burrows, S.R., Buckle, A.M., Clements, C.S., Borg, N.A., Miles, J.J., Beddoe, T., Whisstock, J.C., Wilce, M.C., Silins, S.L., et al. (2005). T cell receptor recognition of a 'super-bulged' major histocompatibility complex class I-bound peptide. Nat. Immunol. *6*, 1114–1122.

Valeva, A., Weisser, A., Walker, B., Kehoe, M., Bayley, H., Bhakdi, S., and Palmer, M. (1996). Molecular architecture of a toxin pore: A 15-residue sequence lines the transmembrane channel of staphylococcal alpha-toxin. EMBO J. *15*, 1857–1864.

Wang, J., Lim, K., Smolyar, A., Teng, M., Liu, J., Tse, A.G., Liu, J., Hussey, R.E., Chishti, Y., Thomson, C.T., et al. (1998). Atomic structure of an alphabeta T cell receptor (TCR) heterodimer in complex with an anti-TCR fab fragment derived from a mitogenic antibody. EMBO J. *17*, 10–26.

Wang, J.-h., Mallis, R.J., and Reinherz, E.L. (2008). Immunodominant-peptide recognition: Beta testing TCR. Immunity *28*, 139–141.